www.nature.com/aps

Acta Pharmacologica Sinica

ARTICLE

Tetrahydroberberrubine retards heart aging in mice by promoting PHB2-mediated mitophagy

Lei Wang[1], Xue-qing Tang[1], Yang Shi[1], Hui-min Li[1], Zi-yu Meng[1], Hui Chen[1], Xiao-han Li[1], Yong-chao Chen[1], Heng Liu[1], Yang Hong[1], Heng-hui Xu[1], Ling Liu[1], Limin Zhao[1], Wei-na Han[2], Xin Liu[1,3] and Yong Zhang[1,3,4]

Heart aging is characterized by left ventricular hypertrophy and diastolic dysfunction, which in turn induces a variety of cardiovascular diseases. There is still no therapeutic drug to ameliorate cardiac abnormities in heart aging. In this study we investigated the protective effects of berberine (BBR) and its derivative tetrahydroberberrubine (THBru) against heart aging process. Heart aging was induced in mice by injection of D-galactose (D-gal, 120 mg · kg^{-1} · d^{-1}, sc.) for 12 weeks. Meanwhile the mice were orally treated with berberine (50 mg · kg^{-1} · d^{-1}) or THBru (25, 50 mg · kg^{-1} · d^{-1}) for 12 weeks. We showed that BBR and THBru treatment significantly mitigated diastolic dysfunction and cardiac remodeling in D-gal-induced aging mice. Furthermore, treatment with BBR (40 μM) and THBru (20, 40 μM) inhibited D-gal-induced senescence in primary neonatal mouse cardiomyocytes in vitro. Overall, THBru exhibited higher efficacy than BBR at the same dose. We found that the levels of mitophagy were significantly decreased during the aging process in vivo and in vitro, THBru and BBR promoted mitophagy with different potencies. We demonstrated that the mitophagy-inducing effects of THBru resulted from increased mRNA stability of prohibitin 2 (PHB2), a pivotal factor during mitophagy, thereby upregulating PHB2 protein expression. Knockdown of PHB2 effectively reversed the antisenescence effects of THBru in D-gal-treated cardiomyocytes. On the contrary, overexpression of PHB2 promoted mitophagy and retarded cardiomyocyte senescence, as THBru did. In conclusion, this study identifies THBru as a potent antiaging medicine that induces PHB2-mediated mitophagy and suggests its clinical application prospects.

Keywords: heart aging; berberine; tetrahydroberberrubine; mitophagy; PHB2; antiaging medicine

Acta Pharmacologica Sinica (2023) 44:332–344; https://doi.org/10.1038/s41401-022-00956-w

INTRODUCTION

Biological aging is associated with a gradual decline in organismal reproductive and regenerative capacity, although dramatic individual variations exist in the rates of decline [1]. By 2050, the population of individuals ≥65 years old is projected to reach 1.6 billion worldwide [2]. However, with a growing aged population, diseases connected to aging are also on the rise. Among them, cardiovascular diseases are the leading cause of death in the elderly population [3]. Heart aging refers to age-related deterioration of cardiac function and manifests as the loss of myocardial contractile capacity, including increased left ventricular (LV) wall thickness and chamber size and prolonged diastole [4, 5], which results in the increased vulnerability to the development of a variety of cardiovascular diseases (e.g., coronary artery disease, atrial fibrillation, and heart failure (HF)) [6, 7]. Consequently, the increases in the incidence and prevalence of age-associated cardiovascular diseases impose a grave global problem for human health and a major financial burden on healthcare systems [8, 9]. It is urgent to explore preventive and therapeutic approaches for heart aging.

To date, many theories have been postulated about the pathogenesis of aging-related diastolic dysfunction, including oxidative stress, DNA damage, telomere shortening, genomic instability, epigenetic disarray, inflammation, apoptosis, mitochondrial dysfunction and autophagy inhibition [10–12]. Autophagy is an evolutionarily conserved process that is critical for cellular homeostasis and survival [13]. In addition, highly selective forms of autophagy specifically target damaged organelles, as indicated by mitophagy-mediated clearance of damaged mitochondria [14]. Mitophagy is enhanced in various longevity models, whereas multiple lines of evidence suggest the gradual dysregulation of mitophagy with aging in animals [15, 16]. Notably, mitochondrial dysfunction and mitophagy are crucial determinants of aging-related disorders, including heart aging [17–19]. Therefore, improving mitophagy by manipulating related molecules and specific drugs is a feasible approach to ameliorate heart aging. Prohibitin 2 (PHB2) has been shown to be an important receptor for the formation of mitophagic machinery distinct from the classic PINK1/Parkin pathway [20, 21]. PHB2 is a necessary component of the mitochondrial prohibitin complex, along with

[1]Department of Pharmacology (the State-Province Key Laboratories of Biomedicine-Pharmaceutics of China, Key Laboratory of Cardiovascular Research, Ministry of Education), College of Pharmacy, Harbin Medical University, Harbin 150081, China; [2]Department of Medicinal Chemistry and Natural Medicine Chemistry, College of Pharmacy, Harbin Medical University, Harbin 150081, China; [3]Research Unit of Noninfectious Chronic Diseases in Frigid Zone, Chinese Academy of Medical Sciences, 2019RU070, Harbin 150081, China and [4]Institute of Metabolic Disease, Heilongjiang Academy of Medical Science, Harbin 150081, China
Correspondence: Xin Liu (freyaliuxin@163.com) or Yong Zhang (hmuzhangyong@hotmail.com)
These authors contributed equally: Lei Wang, Xue-qing Tang, Yang Shi

Received: 31 January 2022 Accepted: 7 July 2022
Published online: 10 August 2022

PHB/PHB1, which is a ring-like macromolecular structure at the inner mitochondrial membrane [22–24]. Some studies have revealed the functional roles of PHB2 in HF, acute kidney injury, and non-small-cell lung carcinoma (NSCLC) [25–27]. However, whether PHB2 is involved in heart aging or acts as an effective therapeutic target is still unknown.

Berberine (BBR) is an isoquinoline alkaloid that was initially derived from *Rhizoma Coptidis*, *Hydrastis canadensis*, and *Berberis aquifolium* [28, 29]. Recent studies have shown that BBR possesses anticancer [30], antineurodegenerative [31], intraperitoneal adhesion [29] and antiaging [32] properties. However, accumulating evidence has revealed the poor drug-like properties of BBR, such as poor absorption in the gut and rapid metabolism within the body [33]. Therefore, studies focusing on the research and development of BBR derivatives with better druggability and fewer side effects are valuable [34–36]. Tetrahydroberberrubine (THBru), a BBR derivative, was created by semichemical synthesis, in which BBR chloride undergoes pyrolysis monodemethylation and then reduction by potassium borohydride [37]. Although the pharmacological effects of THBru have been documented, such as inhibiting inflammation, preventing lung injury and treating anxiety [38–40], the effect of THBru on inhibiting heart aging and the underlying mechanisms have not been studied.

Here, we used in vivo and in vitro models of aging to investigate the pharmacological regulation of PHB2-mediated mitophagy by THBru in heart aging. The efficacies of THBru and BBR were also compared.

MATERIALS AND METHODS

Animals

Six-month-old female C57BL/6N mice were obtained from Beijing Vital River Laboratory Animal Technology Co., Ltd. The mice were under a stable raising condition (temperature, 23 ± 1 °C; humidity, 55%–60%) and had free access to food and drinking water. After acclimation for a week, the mice were randomly divided into six groups as follows: the normal control group (Control), the D-galactose-induced aging group (D-gal), the D-gal group treated with low-dose THBru (25 $mg \cdot kg^{-1} \cdot d^{-1}$, D-gal + THBru-1), the D-gal group treated with high-dose THBru (50 $mg \cdot kg^{-1} \cdot d^{-1}$, D-gal + THBru-2), the D-gal group treated with berberine (50 $mg \cdot kg^{-1} \cdot d^{-1}$, D-gal + BBR) and the D-gal group treated with rapamycin (10 $mg \cdot kg^{-1} \cdot d^{-1}$, D-gal + Rapa). The normal control group with subcutaneous injection of 0.9% saline and the other experiment groups were injected with D-galactose (D-gal, 120 $mg \cdot kg^{-1} \cdot d^{-1}$ in saline, Sigma-Aldrich, MO, USA) as described previously continuously for 12 weeks [41]. The drugs including THBru, BBR and Rapa were administered via gastric gavage for 12 weeks (dissolved in 0.9% saline with 0.5% sodium carboxymethylcellulose). After the measurement of cardiac functions, the mice were anesthetized and sacrificed for measurements of senescent markers and histomorphology analysis.

Reagents

Tetrahydroberberrubine (THBru), obtained from the Department of Pharmaceutical Chemistry, Harbin Medical University. Berberine [1, 8-dihydroxy-3-(hydroxymethyl)-anthraquinone] and rapamycin were purchased from Solarbio Co. (Beijing, China). The structures of THBru and BBR are shown in Fig. S2A, B. In parallel, THBru, BBR and rapamycin were dissolved in dimethyl sulfoxide (DMSO, Sigma, Louis, MO, USA) and stored at 4 °C. The cells were treated with or without THBru (20 or 40 μM), BBR (40 μM) or Rapa (100 nM). Control cells were treated with a non-toxic final concentration of 0.1% DMSO. Rapa was used as positive control. Forty micro molars D-gal was used to induce cell senescence. 3-Methyladenine (3-MA) was purchased from MedChemExpress (HY-19312). And actinomycin D (Act. D) was from MedChemExpress (HY-17559).

Echocardiographic analyses

Transthoracic echocardiography was performed using a Vevo® 2100 High-Resolution Imaging System (VisualSonics, FUJIFILM, Toronto, Canada) ultrasound machine equipped with a 40.0-MHz phase-array transducer. M-mode recordings were performed at the level of the papillary muscles according to the double-blind procedure [42]. LV internal diameters (LVID; s and LVID; d), interventricular septum thickness (IVS; s and IVS; d) and LV posterior wall thickness (LVPW; s and LVPW; d) were each measured during systole and diastole, then EF% and FS% were calculated. echo-Doppler transmitral flow imaging in the apical 4-chamber view was performed by placing the pulsed wave Doppler at the septal corner of the mitral annulus. E peak was determined as peak mitral annular velocity during early filling. And A peak was determined as peak mitral annular velocity during late diastole [43].

Histopathological and morphometric analysis

Hematoxylin and eosin (HE) and Masson's trichrome staining were used to evaluate histopathological changes and collagen distribution. Tissue slices were stained with HE reagents or Masson's trichrome kit which were purchased from Solarbio Co. (Beijing, China). Images were photoed by the light microscope (Carl Zeiss, Germany) and were analyzed using Image J software.

Immunohistology of heart

For immunohistochemical (IHC) analysis, paraformaldehyde-fixed paraffin embedded sections of mouse heart were deparaffinized and rehydrated through serial xylene and ethanol washes, then rinsed in tap water. Endogenous peroxidase was quenched by incubating the sections in 3% in H_2O_2 at room temperature for 10 min. Antigen retrieval was performed by incubation of the tissue in citric acid buffer at 100 °C for 30 min. Sections were stained with anti-PHB2 (Abcam, Cambridge, UK, ab85554, 1:500). Subsequently, sections were incubated with secondary HRP-conjugated antibodies at room temperature for 2 h. In all cases sections from control and experimental groups were analyzed in parallel. The stained slides were counterstained with Haematoxylin, dehydrated through serial ethanol and xylene washes and mounted using DPX (Sigma-Aldrich, USA). IHC images of the heart were captured with a light microscope. In addition, immunofluorescence was performed on frozen heart section and cardiomyocytes for expression of PHB2 and α-actin. α-Actin was used as a myocardial marker. Immunofluorescent (IF) staining was performed as previously described [44]. Confocal fluorescence microscopy (Olympus, Fluoview1000, Tokyo, Japan) was used to capture immunofluorescence images of heart. And quantification of IHC and IF images were performed using Image J software.

Isolation of neonatal mouse ventricular myocytes (NMVMs)

Primary neonatal mice ventricular myocytes (NMVMs) were isolated from 1- to 2-day-old mice heart and seeded in the culture plates as previously described [44, 45].

AC16 cell culture

Human AC16 cell lines were cultured in Dulbecco's Modified Eagle's Medium (DMEM) medium with 10% fetal bovine serum (HyClone, USA) at 37 °C under 5% CO_2.

Transfection of PHB2 siRNA and plasmids

NMVMs and AC16 were transiently transfected with PHB2 plasmids or negative controls (RiboBio Co., China), using Lipofectamine 2000 reagent (Invitrogen, USA) according to the instructions. And PHB2 siRNA was transfected into NMVMs and AC16 by the X-treme GENE Transfection Reagent (Roche, USA). The transfection regents were mixed with Opti-MEM serum-free medium and then added to the cells. Six hours later, the

medium was replaced. And then the cells were treated with or without D-gal or THBru. After 48 h of drugs treatment, the cells were used for other analysis. si-PHB2 (5′-GCTGCCGTCCATTGT TAAT-3′).

Cell counting kit-8 (CCK8) assay
CCK8 (Dojindo, Japan) was used for detection of cell proliferation. NMVMs were treated with THBru or BBR, then plated in a 96-well plate and cultivated for 24 h. And then 10% CCK8 solution was added to the cell culture medium for 1 h incubation at 37 °C. Absorbance at 450 nm was detected using a plate reader.

Cell cycle progression assays
AC16 cells were harvested, centrifuged and fixed with 70% cold alcohol at 4 °C overnight. After that, cells were incubated with RNase and propidium iodide (PI) (Invitrogen, USA) at 4 °C in the dark for 30 min. Finally, cell cycle phases analysis was performed using flow cytometry (BD Bioscience, USA).

RNA extraction and quantitative real-time RT-PCR (qPCR)
Total RNA of cardiomyocytes and heart tissues were extracted by TRIzol reagent (Invitrogen, USA). Integrity of RNAs was assessed by standard denaturing agarose gel electrophoresis. cDNA was synthesized by Reverse Transcription Kit (Toyobo, Japan). Real-time PCR was then performed with SYBR Green (Toyobo, Japan). GAPDH was used as an internal control. The sequences of murine primers:

PHB2: F: 5′-ACCGTGGAAGGCGGTCATA-3′
R: 5′- GGTCTGGCCCGAATGTCATAG-3′
GAPDH: F: 5′-AAGAAGGTGGTGAAGCAGGC-3′
R: 5′- TCCACCACCCAGTTGCTGTA-3′.

Western blot analysis
Cardiomyocytes were harvested after 48 h treatment and lysed in RIPA buffer (Solarbio Co, China). Myocardial tissues were lysed in Total Protein Extraction Kit (Wanlei, China). Proteins were fractionated by SDS-PAGE (10%–12% polyacrylamide gels). Proteins were transferred to nitrocellulose filter membrane (PALL, USA). The samples were then incubated with primary antibodies for PHB2 (Abcam, Rabbit, 1:500), LC3 (Cell Signaling Technology, Rabbit, 1:1000), p62 (Cell Signaling Technology, Rabbit, 1:1000), p16 (Cell Signaling Technology, Rabbit, 1:500), p21 (Cell Signaling Technology, Rabbit, 1:500), p53 (Cell Signaling Technology, Rabbit, 1:500) and GAPDH (Proteintech, Mouse, monoclonal, 1:2000) at 4 °C overnight. The membranes were scaned by Odyssey v1.2 software (LI-COR Biosciences, USA).

mRFP-GFP-LC3 staining
The mRFP-GFP-LC3 adenovirus was obtained from Hanbio (autophagy-adv-mRFP-GFP-LC3-1000, China). The fluorescence depends on the difference in pH between the acidic autolysosome (red) and the neutral autophagosome (green/yellow), and the color of fluorescence enables us to monitor the dynamic changes of the autophagic flux. Then images were obtained by confocal fluorescence microscopy (Carl Zeiss, Germany).

JC-1 staining
Cultured NMVMs were loaded with the ratiometric mitochondrial potential indicator JC-1 (5,5′,6,6′-tetrachloro1,1′,3,3′-tetramethylbenzimidazolylcarbocyanine iodide) (Solarbio Co., China) at 5 μM for 30 min at 37 °C. In viable cells, JC-1 exists as two forms, one is monomer (green), which presents depolarized membrane potentials; the other is aggregate (orange), which presents hyperpolarized membrane potentials. Then 50 nM FCCP was added into cells. 10 min later, the NMVMs were illuminated at 488 nm and the emission was collected between 515–545 nm and 575–625 nm. Images were contributed by Olympus (Fluoview1000, Tokyo, Japan).

Transmission electron microscopy
Tissue specimens were prepared by routine methods [46]. One-micrometer-thick Epon embedded sections were stained with uranyl acetate, followed by lead citrate, and examined by JEOL 1200 electron microscope (JEOL Co., Japan).

Senescence-associated β-galactosidase (SA-β-Gal) staining
A Senescence β-Galactosidase Staining Kit (Cell Signaling Technology, USA) was used to evaluate senescence level. In brief, cells and frozen section of heart tissue were washed with PBS, fixed in 4% paraformaldehyde (Sigma-Aldrich, HT5014), washed, and incubated overnight at 37 °C with staining solution containing X-gal at 1 mg/mL, pH 6.0. Images were captured with a light microscope. And the number of SA-β-Gal-positive cells or area was analyzed using Image J software.

Determination of oxidative stress
Reactive oxygen species (ROS) level in cardiomyocytes was assessed by ROS detect kit (Beyotime, China). Briefly, the agent (10 μM) was added to the cardiomyocytes for 20 min at 37 °C, then cells were observed by a confocal microscope (Zeiss, Germany). ROS levels were represented with fluorescence intensity.

HPLC/ESI-IT-TOF-MS analysis
HPLC/ESI-IT-TOF-MS analysis was performed on an Agilent series 1100 HPLC instrument connected to a Finnigan LCQ Advantage ion trap mass spectrometer (ThermoFisher Scientific, Waltham, MA). Samples were prepared as previously described [47]. Data were processed by Xcalibur 2.0.7 software (ThermoFisher).

Statistical analysis
All values are presented as mean ± SEM. Statistical comparisons were performed by Student's *t*-test between two groups or one-way ANOVA for multiple comparisons. $P < 0.05$ was considered to indicate a significant difference. Data were analyzed using GraphPad Prism 8.0 software.

RESULTS

THBru improves diastolic dysfunction in D-galactose (D-gal)-induced aging mice
We first generated an aging mouse model by subcutaneous injection of D-gal into the nape of the neck for 12 weeks. Different concentrations of THBru and BBR were administered by gavage. Rapamycin (RAPA) is a commonly used autophagy activator that targets mTOR and is an effective antiaging agent in different species. Here, we used RAPA as a positive control drug. Echocardiographic assessment was used to examine the cardiac function of mice in each group. The results suggested that compared with the those of control mice, the E/A peak ratio and the E peak velocity of aging mice were significantly reduced, while the isovolumetric relaxation time (IVRT) was markedly prolonged and LV mass (Fig. 1a–f) was increased. These parameters indicated diastolic dysfunction in D-gal-induced aging mice. However, the administration of THBru (25, 50 mg/kg) and BBR (50 mg/kg) significantly improved diastolic dysfunction in aging mice. Notably, THBru exerted better effects than BBR at the same dose. Systolic function was examined by ejection fraction (EF%) and fractional shortening (FS%). We observed a slight decline in EF% and FS% in aging mice, but the difference was not significant, while THBru, BBR and RAPA had no effects on the two parameters (Fig. 1g, h). Left ventricular end diastolic dimension (LVEDD), left ventricular end systolic dimension (LVESD) and heart rate (~400 bpm) had no significant differences among groups (Supplementary Fig. 1). These results indicated that the D-gal-induced EF preserved HF similar to that in natural aging mice, whereas THBru and BBR could effectively improve diastolic dysfunction in aging mice.

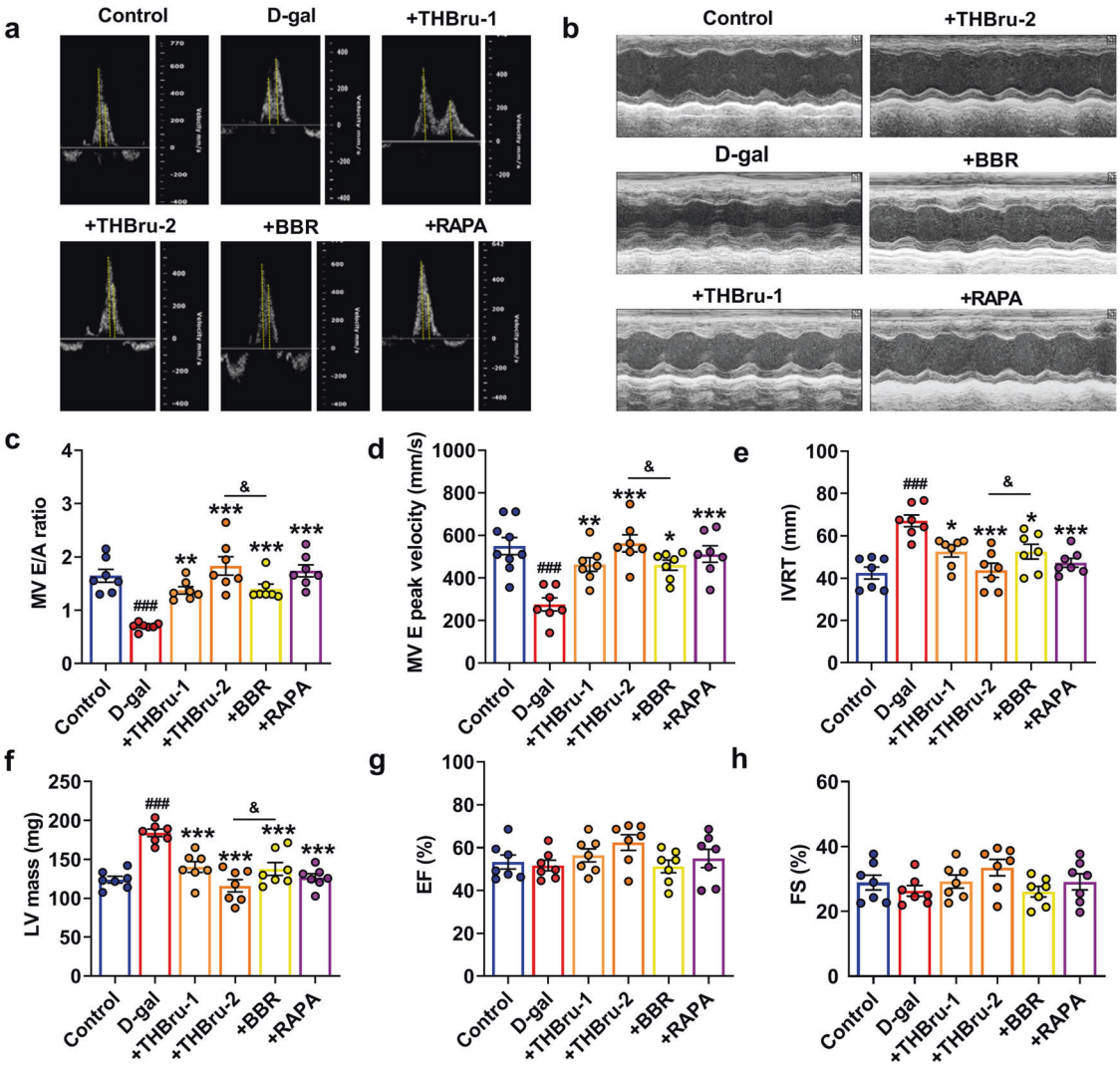

Fig. 1 THBru reduces cardiac diastolic dysfunction in D-gal-induced aging mice. a Representative images of echo-Doppler transmitral flow in aging mice. **b** Representative M-mode echocardiographic images. **c** Statistical results of the E/A ratio. $n = 7$. **d** E peak velocity was quantified. $n = 7$. **e** Statistical results of isovolumetric relaxation time (IVRT). $n = 7$. **f** Data analysis of LV mass (LV mass). $n = 7$. **g** Data analysis of the ejection fraction (EF%). $n = 7$. **h** Data analysis of fractional shortening (FS%). $n = 7$. $^{###}P < 0.001$ vs. control; $^{*}P < 0.05$, $^{**}P < 0.01$, $^{***}P < 0.001$ vs. D-gal; $^{\&}P < 0.05$ between +THBru-2 group vs. +BBR group.

THBru inhibits cardiac remodeling and cardiac senescence in heart aging

To further clarify the effect of THBru in delaying cardiac senescence, HE and Masson staining of mouse heart tissue were performed to detect structural changes and collagen deposition, respectively. The HE staining results showed that after D-gal-induced cardiac senescence, the cardiomyocyte nucleus was enlarged, and the arrangement of myocardial fibers was loose and disordered, while after the administration of THBru and BBR, the arrangement of myocardial fibers was relatively neat and compact, and the size of the nucleus returned to normal (Fig. 2a). The Masson staining results demonstrated that THBru and BBR markedly reduced collagen deposition in the aging heart, but there was a more potent effect in the THBru group (Fig. 2b, d). We further performed β-galactosidase (β-Gal) staining to specifically identify senescent cardiomyocytes. As shown in Fig. 2c, e, the D-gal group showed a marked increase in positive staining of senescence-associated β-Gal. THBru and BBR reduced the positive area of β-Gal labeling induced by D-gal. Next, Western blot was used to measure the expression of the senescence markers p53, p21, and p16 in mouse heart tissues. The results demonstrated that THBru and BBR significantly inhibited the upregulation of these senescence markers in the aging heart (Fig. 2f–h). Moreover, THBru was more effective than BBR in suppressing cardiac senescence at the same dose. These results suggested that THBru and BBR markedly ameliorated cardiac remodeling and cardiomyocyte senescence in aging mice.

THBru inhibits cardiomyocyte senescence

We then examined the effects of THBru and BBR on inhibiting senescence in vitro. In vivo metabolites of THBru were first analyzed by HPLC/ESI-IT-TOF-MS to identify metabolic products. The results suggested that most of the metabolites of THBru in plasma were the primary form ($C_{19}H_{19}NO_4$), and there were small amounts of BBR ($C_{20}H_{18}NO_4$), and tetrahydroberberine ($C_{20}H_{21}NO_4$) (Supplementary Fig. 2, Table 1). Primary neonatal mouse cardiomyocytes were cultured, and D-gal (40 μM) was added to induce cardiomyocytes senescence. We tested the toxic effect of THBru and BBR on cardiomyocytes using CCK8 analysis.

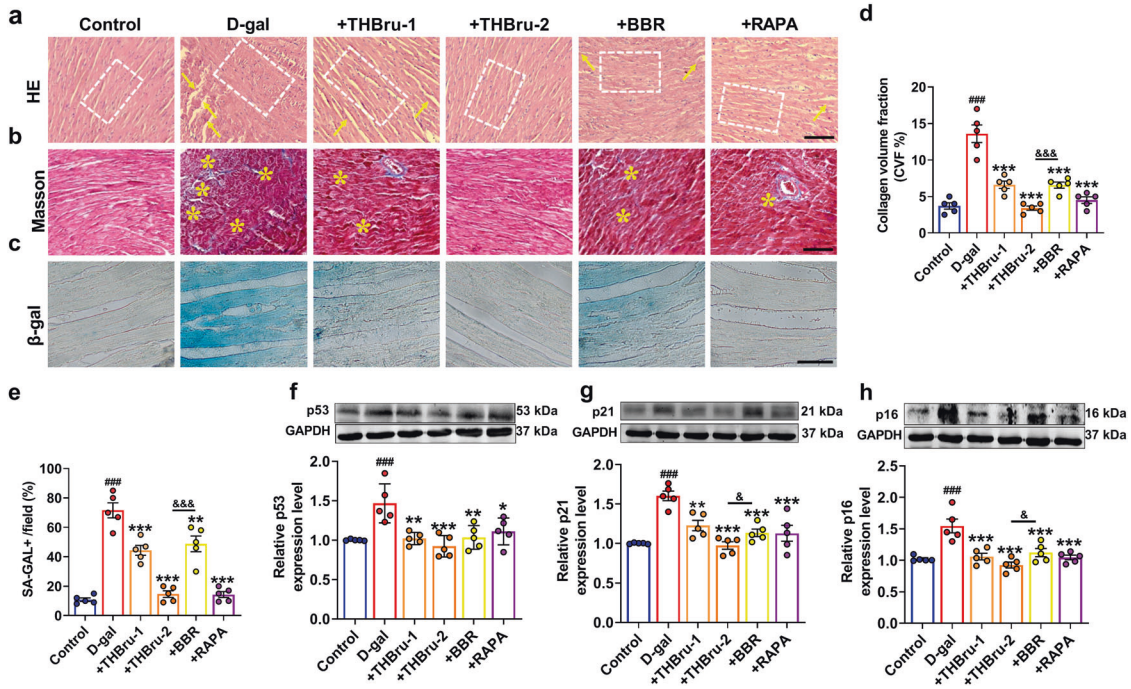

Fig. 2 THBru attenuates cardiac remodeling and delays heart aging in aging mice. a Heart tissue specimens were stained with hematoxylin and eosin (HE) (×400). The arrangement of myocardial fibers is marked by a white dotted box, and the rupture of myocardial fibers is indicated by yellow arrows. $n = 5$. Scale bar: 100 μm. **b** Heart tissue specimens were stained with Masson trichrome dye (×400). The deposition of collagen fibers is indicated by yellow asterisks. $n = 5$. Scale bar: 100 μm. **c** β-gal staining (×200) indicated that THBru delays heart aging. Scale bar: 200 μm. **d** Quantitative analysis of fibrosis, as revealed by Masson trichrome staining. $n = 5$. **e** Quantitative analysis of senescent cardiomyocytes, as revealed by β-gal staining. $n = 5$. **f–h** The expression of p53, p21 and p16 in aging hearts was analyzed by Western blot. $n = 5$. $^{###}P < 0.001$ vs. control; $^{*}P < 0.05$, $^{**}P < 0.01$, $^{***}P < 0.001$ vs. D-gal; $^{\&}P < 0.05$, $^{\&\&\&}P < 0.001$ between +THBru-2 group *vs.* +BBR group.

Table 1. Characterization of in vivo metabolites of tetrahydroberberrubine **1**–**3** by HPLC/ESI-IT-TOF-MS.

No.	RT (min)	Formula	HR-MS $[M+H]^+$			$(+)ESI\text{-}MS^n(m/z)$	Metabolites reaction	Plasma	Urine	Feces
			Measured	Predicted	Δ (ppm)					
1*	6.99	$C_{19}H_{19}NO_4$	326.1394	326.1387	2.15	$MS^2[326]$: 80	None	++	++	++
2	5.50	$C_{20}H_{18}NO_4$	337.1340	337.1309	9.19	$MS^2[337]$: 312, 80	$+CH_3$-4H	—	—	++
3	32.12	$C_{20}H_{20}NO_4$	338.1328	338.1387	9.20	$MS^2[338]$: 321, 312	$+CH_3$	++	++	+

*Identified by comparing with reference standards.
++ detected at high abundance, + detected, — not detected.

The results demonstrated that 100 μM of THBru and BBR had bare of any toxic effect on primary cardiomyocytes. IC_{50} value of THBru and BBR was 1475 μM and 513 μM, which further confirmed the safety of these two compounds with our selected dosages. And the results suggested that THBru had less toxicity than BBR at the same dose (Supplementary Fig. 3). Cell senescence was confirmed by β-Gal staining. The results showed that the number of positively stained cardiomyocytes was increased significantly after D-gal treatment. After treatment with THBru (20, 40 μM), BBR (40 μM) and RAPA (100 nM), cardiomyocyte senescence was markedly inhibited (Fig. 3a, b). It was noted that the high dose of THBru more significantly inhibited senescence than the same dose of BBR. Moreover, the Western blot results suggested that THBru and BBR could reverse the upregulation of p53, p21, and p16 expression caused by D-gal (Fig. 3c–e). We found that THBru more robustly inhibited p21 and p16 expression than BBR, but there was no difference in p53 expression. ROS accumulation is the consequence of oxidative stress and mitochondrial dysfunction during cell senescence. Consistently, our results showed a marked increase in ROS in D-gal-treated cardiomyocytes. Treatment with THBru and BBR decreased D-gal-induced ROS production (Fig. 3f, g). Additionally, THBru more potently inhibited ROS production than BBR. Next, the influence of THBru and BBR on the cell cycle was evaluated in a human cardiomyocyte cell line (AC16) to assess cell senescence. Flow cytometry indicated that the majority of cells were arrested in the G_0/G_1 phase, accompanied by a decrease in the proportion of cells in the S or G_2/M phase in the D-gal-treated group, and this effect was reversed by different doses of THBru and BBR (Fig. 3h, i).

THBru ameliorates defective mitophagy in aging

To clarify the underlying mechanism by which THBru delays heart aging, we first observed ultrastructural changes in the heart tissues in each group by transmission electron microscopy. In D-gal-induced aging mice, myofilament breakage, lipofuscin deposition, nuclear pyknosis, mitochondrial swelling and damage

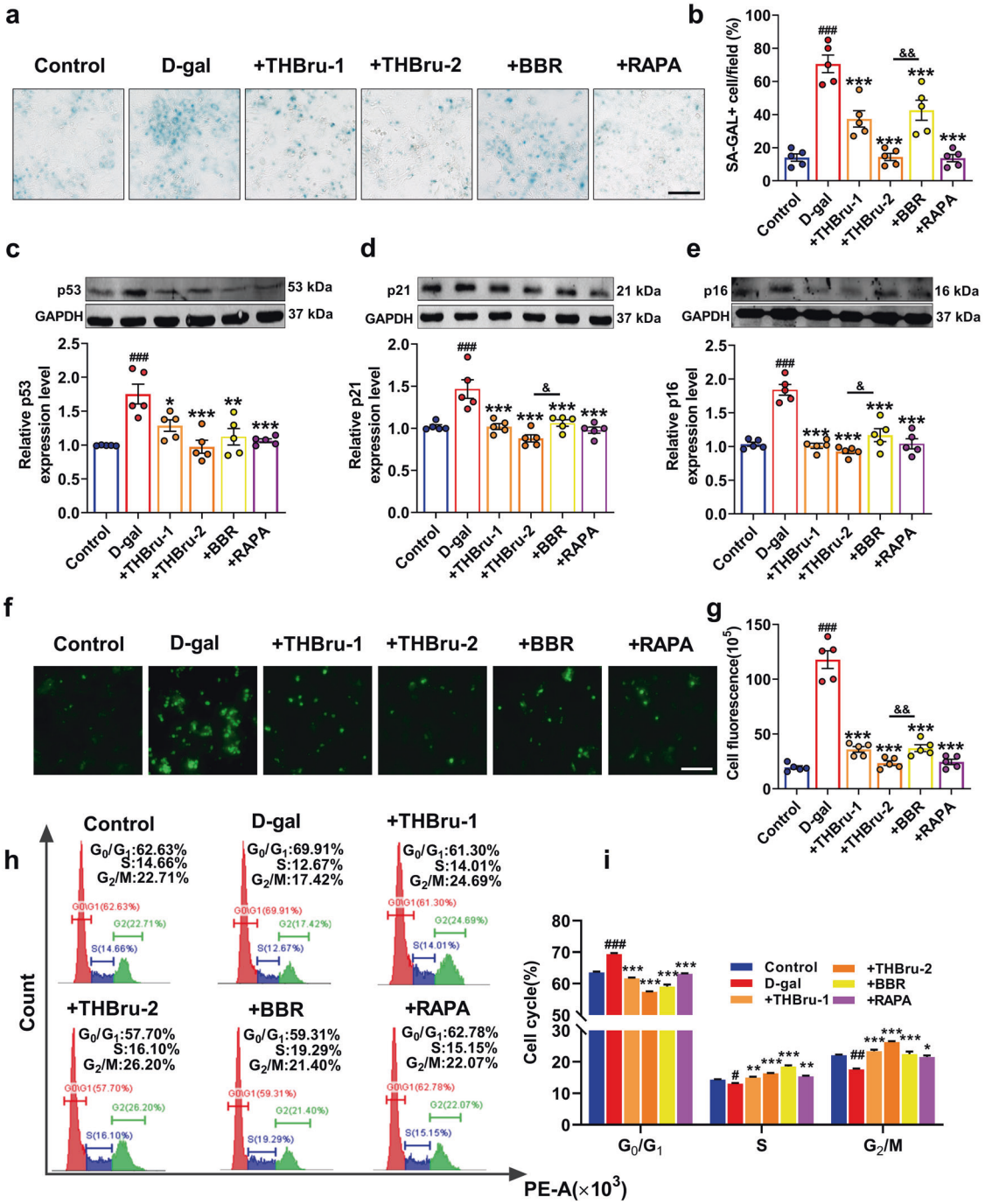

Fig. 3 THBru inhibits cardiomyocyte senescence. a The repressive effects of THBru on the senescence of primary neonatal mouse cardiomyocytes were assessed by β-gal staining (×200). Scale bar: 100 μm. **b** Quantitative analysis of β-gal staining. $n = 5$. **c**–**e** The expression of p53, p21 and p16 in primary neonatal mouse cardiomyocytes was analyzed by Western blot. $n = 5$. **f** ROS levels were measured in primary neonatal mouse cardiomyocytes. Scale bar: 50 μm. **g** Quantitative analysis of ROS levels. $n = 5$. **h** Flow cytometry was used to examine the cell cycle distribution of AC16 cells following D-gal treatment or cotreatment with THBru, BBR and RAPA. **i** Quantitative analysis of flow cytometry. $n = 5$. $^{\#}P < 0.05$, $^{\#\#}P < 0.01$, $^{\#\#\#}P < 0.001$ vs. control; $^{*}P < 0.05$, $^{**}P < 0.01$, $^{***}P < 0.001$ vs. D-gal; $^{\&}P < 0.05$, $^{\&\&}P < 0.01$ between +THBru-2 group vs. +BBR group.

were obviously observed. Moreover, defective mitophagy was also observed in the D-gal group. THBru and BBR administration ameliorated these ultrastructural injuries and markedly increased mitophagy, similar to the effect of RAPA (Fig. 4a). The expression of the autophagy-related proteins LC3 and p62 was also measured in the heart tissues in each group of mice. The results demonstrated that THBru and BBR significantly downregulated the expression of p62 and simultaneously upregulated the ratio of LC3-II/LC3-I (Fig. 4b, c), which indicated the activation of mitophagy by THBru and BBR. We further verified mitophagy in cardiomyocytes. mRFP-GFP-LC3 double-labeled adenovirus staining was used to measure the level of autophagic flux, and the results showed that THBru and BBR markedly reversed the decrease in autophagic flux in cardiomyocytes caused by D-gal

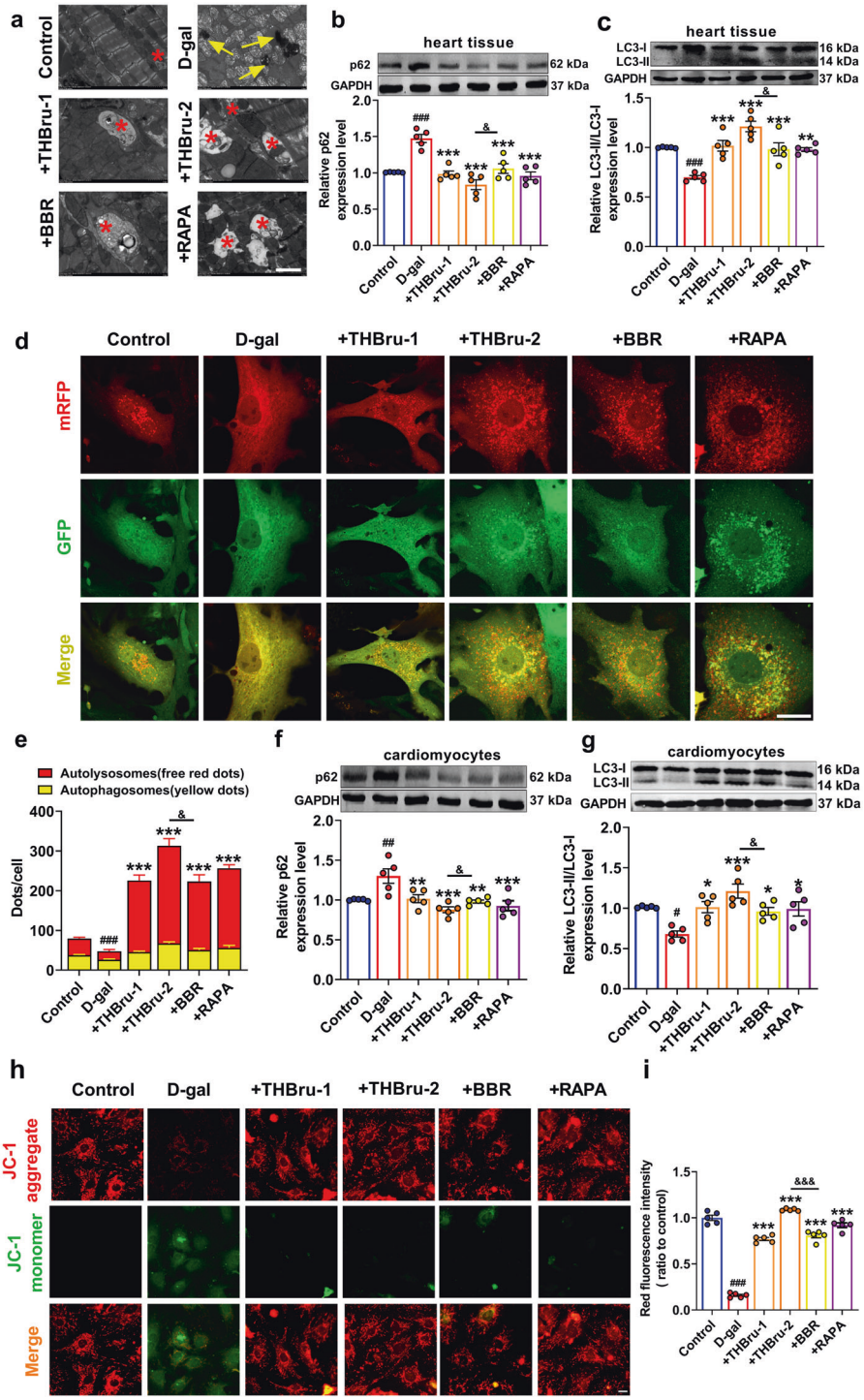

Fig. 4 **THBru promotes mitophagy in vitro and in vivo. a** The alterations in mitochondria and autophagy in cardiac tissue were examined by transmission electron microscopy (TEM). Lipofuscin is indicated by yellow arrows, and autophagosomes are marked by red asterisks. Scale bars: 2 μm. $n = 5$. **b**, **c** The expression of p62 and LC3 in aging hearts was analyzed by Western blot. $n = 5$. **d** Representative images of mRFP-GFP double-labeled adenovirus staining denoting the level of autophagic flux. Yellow puncta denote autophagosomes, and red puncta denote autolysosomes in the merged images. The average numbers of cells were analyzed. Scale bars: 12.5 μm. **e** Quantitative analysis of mRFP-GFP-LC3 staining. $n = 5$. **f**, **g** The expression of p62 and LC3 in primary neonatal mouse cardiomyocytes was analyzed by Western blot. $n = 5$. **h** Representative images of JC-1 staining. The green staining of the JC-1 monomer seen under D-gal treatment indicates depolarization of the $\Delta\Psi m$, and red staining of the JC-1 polymer marks mitochondria. Scale bars: 20 μm. **i** Quantitative analysis of JC-1 staining. $n = 5$. $^{\#}P < 0.05$, $^{\#\#}P < 0.01$, $^{\#\#\#}P < 0.001$ vs. control; $^{*}P < 0.05$, $^{**}P < 0.01$, $^{***}P < 0.001$ vs. D-gal; $^{\&}P < 0.05$, $^{\&\&\&}P < 0.001$ between +THBru-2 group *vs.* +BBR group.

(Fig. 4d, e). Moreover, both THBru and BBR inhibited p62 protein levels but increased LC3-II/LC3-I protein levels in D-gal-treated cardiomyocytes (Fig. 4f, g). The mitochondrial permeability transition (MPT) indicates mitophagy [48]. We next examined whether THBru and BBR could alleviate the D-gal-induced decline in mitochondrial membrane potential (ΔΨm) by JC-1 staining. As shown in Fig. 4h, i, THBru and BBR inhibited the loss of ΔΨm and significantly increased the ratio of the fluorescence intensity. THBru-mediated mitophagy promotion was more potent than that of BBR in both D-gal-induced heart aging and senescent cardiomyocytes. We also confirmed the regulatory effects of THBru and BBR on mitophagy activation and senescence suppression under the condition of autophagosome clearance by 3-MA. The results demonstrated that THBru and BBR could effectively increase mitophagy and inhibit cardiomyocyte senescence even after 3-MA (100 mM) pretreatment (Supplementary Figs. 4 and 5).

THBru upregulates the expression of PHB2 by stabilizing PHB2 mRNA in heart aging

The mitophagy-promoting effect of BBR has been verified in many published studies. Therefore, we focused on the molecular mechanism by which THBru but not BBR activates mitophagy. Studies have shown that PHB2 plays an important role in the regulation of mitophagy [21]. When mitochondria are damaged, the outer mitochondrial membrane ruptures, and the mitochondrial inner membrane protein PHB2 is exposed. The autophagy adapter molecule p62 then recruits and binds with LC3, which promotes the formation of autophagosomes to clear damaged mitochondria [23]. However, the functional role of PHB2 in heart aging has not been revealed. We first proved that PHB2 overexpression in D-gal-treated cardiomyocytes significantly inhibited senescence, as indicated by the decrease in β-gal-positive cells (Supplementary Fig. 6a–c, e), as well as p53, p21 and p16 protein levels (Supplementary Fig. 6g–i). In addition, PHB2 also reversed ROS production (Supplementary Fig. 6d, f) and cell cycle arrest (Supplementary Fig. 6j, k) in senescent cardiomyocytes. Mitophagy was also markedly activated by PHB2 overexpression (Supplementary Fig. 7). Next, we examined whether PHB2 mediated THBru-induced mitophagy promotion in heart aging. The qRT–PCR and Western blot results showed that the expression of PHB2 in the aging heart was significantly reduced while increased after THBru treatment (Fig. 5a, b). Immunofluorescence and immunohistochemical staining of heart tissue sections also confirmed this conclusion (Fig. 5c–e). Consistently, we found that THBru increased PHB2 mRNA and protein expression levels in D-gal-treated cardiomyocytes but not in normal condition (Supplementary Fig. 8). mRNA stability is one of the most important factors contributing to protein expression levels. Actinomycin D (Act. D) was used to block transcription to examine RNA stability in cardiomyocytes. The mRNA levels of PHB2 were measured at different time points (0, 8, 16, and 24 h). The results suggested that THBru treatment markedly delayed mRNA degradation compared to that in the control group, resulting in a prolonged half-life (Fig. 5f, g). These results revealed that THBru increased PHB2 expression by stabilizing PHB2 mRNA.

Knockdown of PHB2 reverses THBru-mediated senescence inhibition in heart aging

To further verify whether THBru-mediated inhibition of heart aging depends on PHB2, we examined the effect of PHB2 knockdown on mitophagy activation and senescence inhibition in the presence of THBru. PHB2 mRNA and protein levels were significantly inhibited by PHB2 siRNA (+si-PHB2) transfection, which also diminished THBru-mediated upregulation of PHB2 expression (Fig. 6a, b). Moreover, si-PHB2 inhibited THBru-mediated promotion of LC3-II/LC3-I and increased p62 levels (Fig. 6c, d). The mRFP-GFP double-labeled adenovirus staining results also showed that knocking down PHB2 abrogated the increase in autophagic flux induced by THBru (Fig. 6e, f), suggesting that si-PHB2 attenuated THBru-mediated mitophagy induction during cardiomyocyte senescence. We then tested the impact of si-PHB2 on cardiomyocyte senescence. As shown in Fig. 7a–d, the β-gal staining results suggested that PHB2 knockdown suppressed the protective effects of THBru on cardiomyocyte senescence and ROS production. The senescence markers p53, p21 and p16 were also upregulated after si-PHB2 transfection (Fig. 7e–g). Moreover, cell cycle arrest in senescent cardiomyocytes was ameliorated by THBru and was reversed by PHB2 knockdown, as indicated by an increased proportion of cardiomyocytes in G_0/G_1 phase, accompanied by a decrease in the proportion of cells in S or G_2/M phase (Fig. 7h, i). These results demonstrated that THBru inhibited cardiomyocyte senescence by targeting PHB2.

DISCUSSION

Cardiovascular diseases are the leading cause of death in the aging population [49]. Pathological damage to the aging heart has been thoroughly characterized, but the underlying molecular mechanisms and effective therapeutic drugs still need further investigation. The aims of this research were to elucidate the protective effect of THBru, a modification of the traditional Chinese medicine BBR, on heart aging and its underlying mechanism. Our data demonstrated that THBru improved cardiac function and remodeling in aging mice. Mechanistically, THBru promoted PHB2-mediated mitophagy and reduced the accumulation of ROS, which contributed to the clearance of damaged mitochondria in the aging heart. Moreover, THBru increased the PHB2 expression level by stabilizing PHB2 mRNA.

Cardiac and vascular aging prominently affect diastolic function [50]. LV diastolic stiffness increases with age in humans, even in the absence of hypertension [51]. A similar pathological condition of heart diastolic dysfunction was observed in the aging mouse model in our current study. Moreover, structural remodeling is strongly linked to cardiac dysfunction in heart aging, which is in agreement with our experimental results, indicating cardiac hypertrophy, interstitial and subendocardial fibrosis, and amyloid deposition [52]. THBru and BBR effectively improve diastolic dysfunction in aging mice by ameliorating adverse cardiac remodeling and cardiac senescence.

In recent years, several compounds have been identified that inhibit heart aging. Prior studies have established a link between the mTOR signaling pathway and aging in organisms ranging from yeast to mammals [53]. RAPA, a small molecule inhibitor of the protein kinase mTOR, can extend the lifespan of model organisms, including mice [54], but its utility is limited by considerable side effects, including metabolic dysfunction, cataracts, and testicular atrophy [55]. Oral supplements of the natural polyamine spermidine have been shown to extend the lifespan of mice by enhancing cardiac autophagy and mitochondrial respiration, as well as improving the diastolic function in the heart in aging mice [56]. Recently, compounds that elevate NAD^+, including nicotinamide mononucleotide (NMN), nicotinamide riboside (NR), and P7C3, have been proposed as possible therapeutics for preventing several age-related pathologies [57–60]. In addition, many antiaging drugs with great potential have also been identified in Chinese herbal extracts. For example, resveratrol can improve oxidative stress and thereby further delay heart aging [61]. To date, there have been no clinical studies to identify the effect of novel targeted agents on heart aging. There is still a huge need for more candidates in this area. Our current research compared the effects of THBru and BBR on inhibiting heart aging. BBR, which is as an effective ingredient in the traditional Chinese medicine Coptis, exhibits

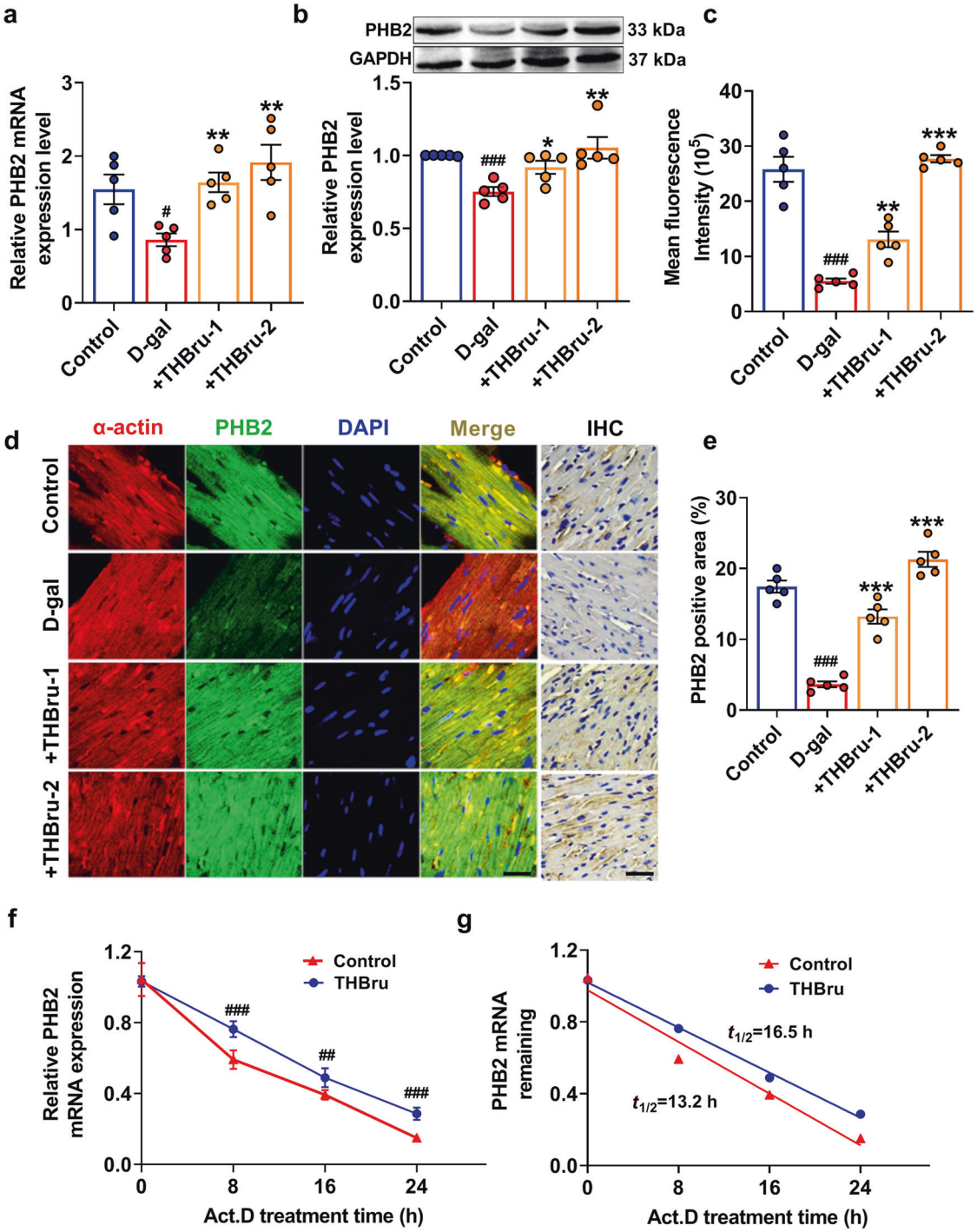

Fig. 5 THBru increases the expression of PHB2 by stabilizing PHB2 mRNA in aging hearts. a PHB2 mRNA levels were examined by qRT–PCR. $n = 5$. **b** PHB2 protein levels were measured by Western blot. $n = 5$. **c** Quantitative analysis of PHB2 immunofluorescence. $n = 5$. **d** Immunofluorescence and immunohistochemical staining of heart tissue were performed to assess the expression of PHB2 in aging hearts. Scale bars: 10 μm, 2 μm. **e** Statistical results of the PHB2-positive area, as shown by immunohistochemical staining. $n = 5$. **f** Primary neonatal mouse cardiomyocytes were treated with Act. D for the indicated times, and PHB2 mRNA levels were measured by qPCR. $n = 5$. **g** Statistical results revealing the stability of PHB2 in neonatal mouse cardiomyocytes. $n = 5$. $^{\#\#}P < 0.01$, $^{\#\#\#}P < 0.001$ vs. control; $^{*}P < 0.05$, $^{**}P < 0.01$, $^{***}P < 0.001$ vs. D-gal.

many biological activities. Studies have shown that BBR has potential antiaging functions [32]. However, its low water solubility and low bioavailability have greatly restricted its clinical application. The bioavailability of its derivative THBru, on the other hand, is much higher than that of BBR, but research on the pharmacological mechanism and function of THBru is in its infancy. Previous studies have demonstrated that THBru has anxiolytic effects and does not produce excitatory or inhibitory effects on the central nervous system [40]; therefore, it is expected to become a candidate for inhibiting anxiety. Moreover, THBru can also effectively inhibit the release of inflammatory factors and improve acute lung injury [39]. Its

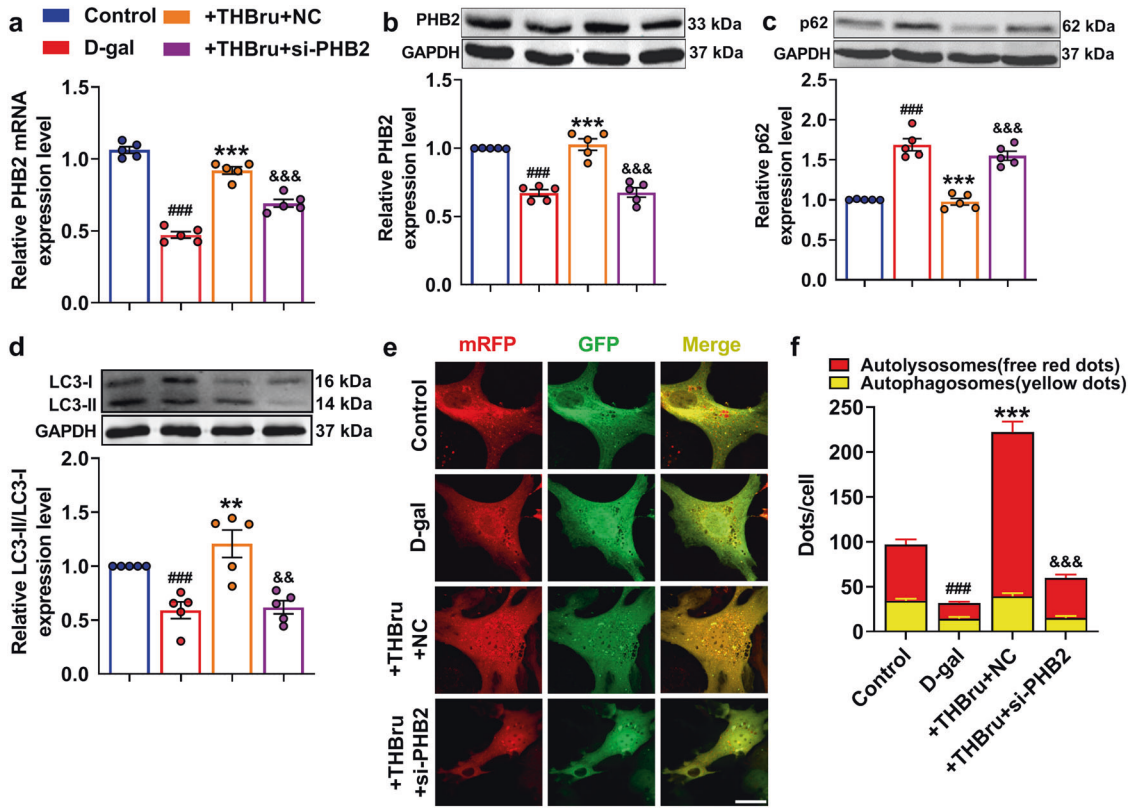

Fig. 6 Knockdown of PHB2 attenuates mitophagy activated by THBru. a PHB2 mRNA levels were measured by qRT–PCR to verify the transfection efficiency of si-PHB2. $n = 5$. **b** PHB2 protein levels were measured by Western blot. $n = 5$. **c**, **d** p62 and LC3 protein levels in primary neonatal mouse cardiomyocytes were measured by Western blot. $n = 5$. **e** PHB2 knockdown delays autophagic flux, as indicated by GFP-mRFP double-labeled adenovirus staining. The average numbers of cells were analyzed. Scale bars: 12.5 μm. **f** Quantitative analysis of mRFP-GFP-LC3 staining. $n = 5$. $^{###}P < 0.001$ vs. control; $^{**}P < 0.01$, $^{***}P < 0.001$ vs. D-gal; $^{\&\&}P < 0.01$, $^{\&\&\&}P < 0.001$ vs. +THBru + NC.

mechanism is related to the MAPK, AKT, and NF-κB signaling pathways [39]. However, currently, there is no evidence suggesting that THBru has antiaging effects on the heart, and its mechanism of action and clinical applications have yet to be explored. The results of our study demonstrated that THBru was more effective than BBR in protecting against heart aging in vitro and in vivo. The differences in diastolic function and cardiac remodeling were characterized by amelioration of the E/A ratio, E peak velocity, IVRT, and LV mass with echocardiography; downregulation of the expression of the aging-related genes p21 and p16; a reduction in positive β-gal staining; and decreased collagen accumulation. At the cellular level, a differential treatment effect was also observed in ROS accumulation and cell cycle arrest.

Mitophagy is a form of selective autophagy that can eliminate damaged mitochondria, which is essential for maintaining the normal physiological processes of cells [62]. Recent studies have shown that defective mitophagy is highly linked to aging and age-related diseases [18], including neurodegenerative diseases, arrhythmia, myocardial infarction, and HF [63]. Due to the indivisibility of cardiomyocytes, they are highly dependent on mitophagy to renew damaged mitochondria [64]. Therefore, targeting mitophagy is a promising therapeutic strategy for cardiovascular diseases, especially aging-related heart dysfunction. Previous studies have shown that compared with wild-type mice, heart-specific SIRT3-knockout mice showed obvious heart aging phenotypes, such as cardiac hypertrophy and diastolic dysfunction [65]. Long-term mitophagy deficiency might be the reason. In this study, we found that the level of mitophagy in the heart tissue of aging mice induced by D-gal was decreased. However, THBru and BBR administration effectively induced mitophagy activation in senescent cardiomyocytes. Consistent with phenotypic changes in senescence, THBru was more beneficial in activating mitophagy and in autophagosome formation and autolysosome fission than BBR. This phenomenon might explain the discrepancy in the overall effects of the two treatments. The reason for the difference in the effects is not completely clear.

PHB2 is a highly conserved scaffold protein located in the mitochondrial inner membrane that forms the mitochondrial prohibitin complex along with PHB/PHB1 [24]. Recent studies have identified PHB2 as a direct receptor for LC3 in the mitophagic machinery [23]. PHB2 binds the autophagosomal membrane-associated protein LC3 through an LC3-interaction region (LIR) domain upon mitochondrial depolarization and proteasome-dependent outer membrane rupture, and it is required for the clearance of paternal mitochondria [23]. Our study first demonstrated that PHB2 could prevent cardiomyocyte senescence by inducing mitophagy. In addition, several studies have also shown that PHB2 might be a novel drug target for diseases associated with defective mitophagy. Yan et al. found that the small molecule compound FL3 could inhibit the function of PHB2 by binding to PHB2 and thereby significantly block the mitophagy pathway to exert antitumor effects [24]. A number of in-depth studies have revealed the mechanism by which BBR activates mitophagy; thus, we focused on the biomolecular mechanism of THBru-induced mitophagy. Our study supports a role for THBru in maintaining mitochondrial quality control by affecting PHB2 expression. A strong inhibitory effect of THBru on PHB2 was observed at both the mRNA and protein levels. Moreover, the stabilization of PHB2 mRNA might be responsible for the positive effect of THBru on

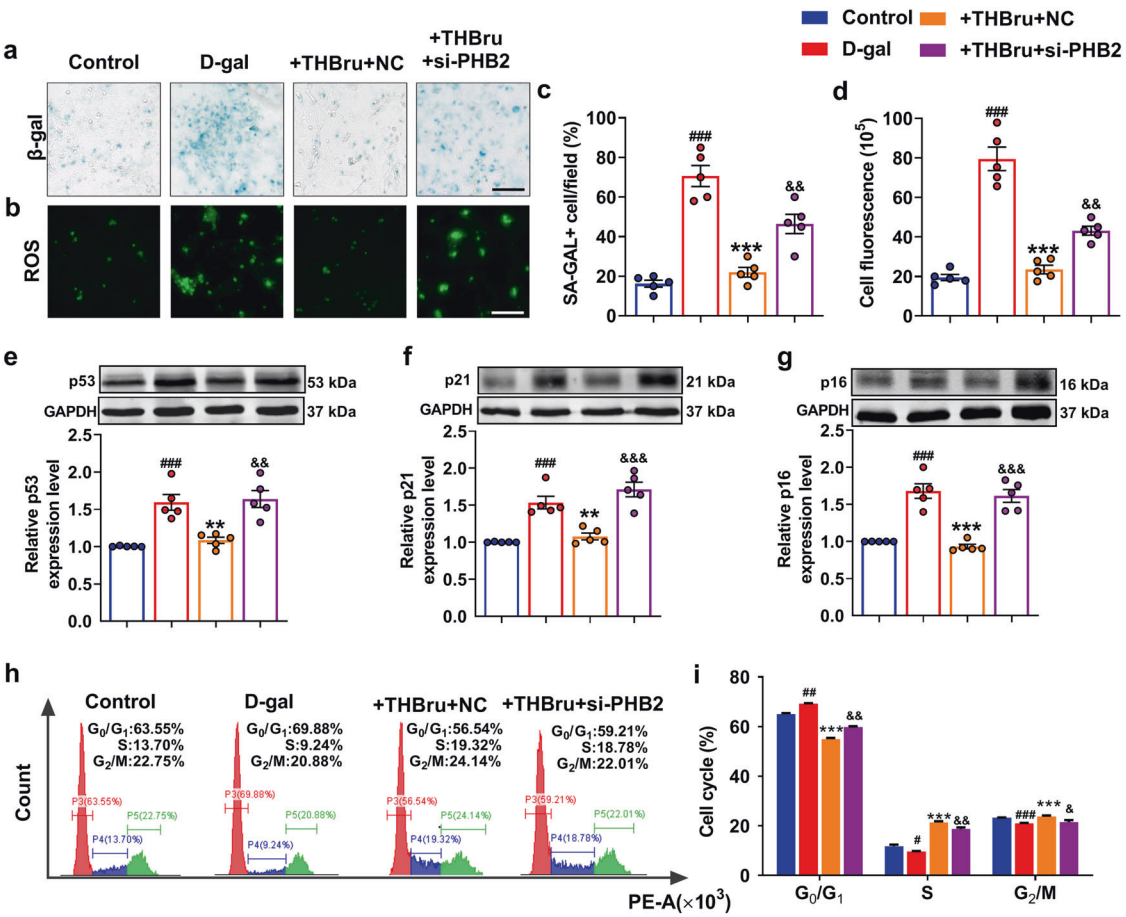

Fig. 7 **PHB2 plays a pivotal role in the antiaging effect of THBru. a** Primary neonatal mouse cardiomyocytes were transfected with si-PHB2 and then examined by β-gal staining (×200). Scale bar: 100 μm. **b** Primary neonatal mouse cardiomyocytes were transfected with si-PHB2, and the production of ROS was measured. Scale bar: 50 μm. **c** Quantitative analysis of β-gal staining. $n = 5$. **d** Quantitative analysis of ROS levels. $n = 5$. **e**–**g** The expression of p53, p21 and p16 in primary neonatal mouse cardiomyocytes was analyzed by Western blot. $n = 5$. **h** The cell cycle was examined by flow cytometry. **i** Quantitative analysis of flow cytometry. $n = 5$. $^{\#}P < 0.05$, $^{\#\#}P < 0.01$, $^{\#\#\#}P < 0.001$ vs. control; $^{**}P < 0.01$, $^{***}P < 0.001$ vs. D-gal; $^{\&}P < 0.05$, $^{\&\&}P < 0.01$, $^{\&\&\&}P < 0.001$ *vs.* +THBru + NC.

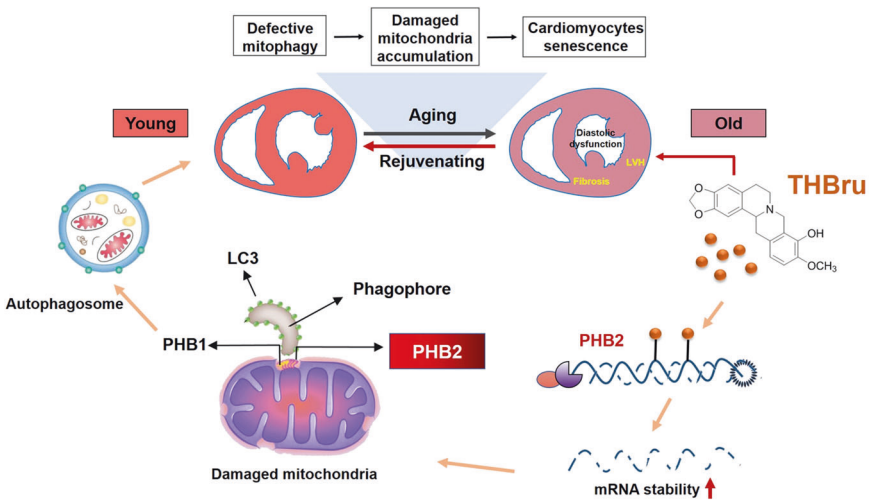

Fig. 8 Underlying mechanisms of the protective effect of THBru against heart aging.

PHB2 expression. This finding suggests that PHB2 is a potential drug target for THBru and might become a promising antiaging target. The role of THBru in the regulation of PHB2 mRNA stability may be an exciting area for further investigation.

In conclusion, our study proved that THBru and BBR improved cardiac remodeling and cardiac dysfunction during the heart aging process. THBru prevented heart aging by increasing PHB2-mediated mitophagy (Fig. 8). Moreover, THBru exhibited a more

potent anti-heart aging effect than BBR. Therefore, our data suggest that THBru might be a promising therapeutic compound to improve cardiac function in aging.

DATA AVAILABILITY

The data that support the findings of this study are available from the corresponding author upon request.

ACKNOWLEDGEMENTS

We thank Qi Wang, Zhi-xia Wang, Hao Cui and Bo Peng for their advice to the study. This work was supported by the National Natural Science Foundation of China (81773735, 81903610, 91949130, 81961138018), National Key R&D Program of China (2017YFC1702003) and HMU Marshal Initiative Funding (HMUMIF-21022).

AUTHOR CONTRIBUTIONS

YZ and XL conceived and designed the study. LW, XQT, YS performed major experiments, drafted the manuscript and analyzed the data. HML, ZYM, and HC performed Western blot, immunochemistry, and qPCR experiments. XHL, YCC, HL, and YH performed primary cell culture and transfection experiments. LMZ, HHX, and LL performed animal experiments. WNH synthesized THBru and analyzed the data. All authors edited the manuscript and approved the final manuscript.

FUNDING

This study was funded by the National Natural Science Foundation of China (91949130, 81961138018, 81903610) and HMU Marshal Initiative Funding (HMUMIF-21022).

ADDITIONAL INFORMATION

Supplementary information The online version contains supplementary material available at https://doi.org/10.1038/s41401-022-00956-w.

Competing interests: The authors declare no competing interests.

Ethics approval: All procedures were approved by the Institutional Animal Care and Use Committee of Harbin Medical University [Protocol (2009)-11]. The use of animals was compliant with the Guide for the Care and Use of Laboratory Animals published by the US National Institutes of Health (NIH Publication No. 85-23, revised 1996). All sacrifices were performed under anesthesia, and every effort was made to minimize animal suffering.

REFERENCES

1. Khan SS, Singer BD, Vaughan DE. Molecular and physiological manifestations and measurement of aging in humans. Aging Cell. 2017;16:624–33.
2. Ferrucci L, Gonzalez-Freire M, Fabbri E, Simonsick E, Tanaka T, Moore Z, et al. Measuring biological aging in humans: a quest. Aging Cell. 2020;19:e13080.
3. Mensah GA, Roth GA, Fuster V. The global burden of cardiovascular diseases and risk factors: 2020 and beyond. J Am Coll Cardiol. 2019;74:2529–32.
4. Obas V, Vasan RS. The aging heart. Clin Sci. 2018;132:1367–82.
5. Liguori I, Russo G, Curcio F, Bulli G, Aran L, Della-Morte D, et al. Oxidative stress, aging, and diseases. Clin Interv Aging. 2018;13:757–72.
6. Paneni F, Diaz Cañestro C, Libby P, Lüscher TF, Camici GG. The aging cardiovascular system: understanding it at the cellular and clinical levels. J Am Coll Cardiol. 2017;69:1952–67.
7. Horn MA, Trafford AW. Aging and the cardiac collagen matrix: Novel mediators of fibrotic remodelling. J Mol Cell Cardiol. 2016;93:175–85.
8. Dunbar SB, Khavjou OA, Bakas T, Hunt G, Kirch RA, Leib AR, et al. Projected costs of informal caregiving for cardiovascular disease: 2015 to 2035: a policy statement from the American Heart Association. Circulation. 2018;137:e558–77.
9. Guzman-Castillo M, Ahmadi-Abhari S, Bandosz P, Capewell S, Steptoe A, Singh-Manoux A, et al. Forecasted trends in disability and life expectancy in England and Wales up to 2025: a modelling study. Lancet Public Health. 2017;2:e307–13.
10. Calcinotto A, Kohli J, Zagato E, Pellegrini L, Demaria M, Alimonti A. Cellular senescence: aging, cancer, and injury. Physiol Rev. 2019;99:1047–78.
11. Kubben N, Misteli T. Shared molecular and cellular mechanisms of premature ageing and ageing-associated diseases. Nat Rev Mol Cell Biol. 2017;18:595–609.
12. Sen P, Shah PP, Nativio R, Berger SL. Epigenetic mechanisms of longevity and aging. Cell. 2016;166:822–39.
13. Mizushima N. Autophagy: process and function. Genes Dev. 2007;21:2861–73.
14. Sica V, Galluzzi L, Bravo-San Pedro JM, Izzo V, Maiuri MC, Kroemer G. Organelle-specific initiation of autophagy. Mol Cell. 2015;59:522–39.
15. Hansen M, Rubinsztein DC, Walker DW. Autophagy as a promoter of longevity: insights from model organisms. Nat Rev Mol Cell Biol. 2018;19:579–93.
16. Nakamura S, Oba M, Suzuki M, Takahashi A, Yamamuro T, Fujiwara M, et al. Suppression of autophagic activity by Rubicon is a signature of aging. Nat Commun. 2019;10:847.
17. Ren J, Zhang Y. Targeting autophagy in aging and aging-related cardiovascular diseases. Trends Pharmacol Sci. 2018;39:1064–76.
18. Ajoolabady A, Aslkhodapasandhokmabad H, Aghanejad A, Zhang Y, Ren J. Mitophagy receptors and mediators: therapeutic targets in the management of cardiovascular ageing. Ageing Res Rev. 2020;62:101129.
19. Onishi M, Yamano K, Sato M, Matsuda N, Okamoto K. Molecular mechanisms and physiological functions of mitophagy. EMBO J. 2021;40:e104705.
20. Lahiri V, Klionsky DJ. PHB2/prohibitin 2: an inner membrane mitophagy receptor. Cell Res. 2017;27:311–2.
21. Wei Y, Chiang WC, Sumpter R Jr, Mishra P, Levine B. Prohibitin 2 is an inner mitochondrial membrane mitophagy receptor. Cell. 2017;168:224–38.e10.
22. Artal-Sanz M, Tavernarakis N. Prohibitin and mitochondrial biology. Trends Endocrinol Metab. 2009;20:394–401.
23. Xiao Y, Zhou Y, Lu Y, Zhou K, Cai W. PHB2 interacts with LC3 and SQSTM1 is required for bile acids-induced mitophagy in cholestatic liver. Cell Death Dis. 2018;9:160.
24. Yan C, Gong L, Chen L, Xu M, Abou-Hamdan H, Tang M, et al. PHB2 (prohibitin 2) promotes PINK1-PRKN/Parkin-dependent mitophagy by the PARL-PGAM5-PINK1 axis. Autophagy. 2020;16:419–34.
25. Huo S, Shi W, Ma H, Yan D, Luo P, Guo J, et al. Alleviation of inflammation and oxidative stress in pressure overload-induced cardiac remodeling and heart failure via IL-6/STAT3 inhibition by raloxifene. Oxid Med Cell Longev. 2021;2021:6699054.
26. Wang J, Zhu P, Li R, Ren J, Zhang Y, Zhou H. Bax inhibitor 1 preserves mitochondrial homeostasis in acute kidney injury through promoting mitochondrial retention of PHB2. Theranostics. 2020;10:384–97.
27. Zhang H, Yin C, Liu X, Bai X, Wang L, Xu H, et al. Prohibitin 2/PHB2 in parkin-mediated mitophagy: a potential therapeutic target for non-small cell lung carcinoma. Med Sci Monit. 2020;26:e923227.
28. Zhang Y, Li X, Zhang Q, Li J, Ju J, Du N, et al. Berberine hydrochloride prevents postsurgery intestinal adhesion and inflammation in rats. J Pharmacol Exp Ther. 2014;349:417–26.
29. Liu X, Wei Y, Bai X, Li M, Li H, Wang L, et al. Berberine prevents primary peritoneal adhesion and adhesion reformation by directly inhibiting TIMP-1. Acta Pharm Sin B. 2020;10:812–24.
30. Ortiz LM, Lombardi P, Tillhon M, Scovassi AI. Berberine, an epiphany against cancer. Molecules. 2014;19:12349–67.
31. Ahmed T, Gilani AU, Abdollahi M, Daglia M, Nabavi SF, Nabavi SM. Berberine and neurodegeneration: A review of literature. Pharmacol Rep. 2015;67:970–9.
32. Dang Y, An Y, He J, Huang B, Zhu J, Gao M, et al. Berberine ameliorates cellular senescence and extends the lifespan of mice via regulating p16 and cyclin protein expression. Aging Cell. 2020;19:e13060.
33. Jin Y, Khadka DB, Cho WJ. Pharmacological effects of berberine and its derivatives: a patent update. Expert Opin Ther Pat. 2016;26:229–43.
34. Li YH, Li Y, Yang P, Kong WJ, You XF, Ren G, et al. Design, synthesis, and cholesterol-lowering efficacy for prodrugs of berberrubine. Bioorg Med Chem. 2010;18:6422–8.
35. Cheng Z, Chen AF, Wu F, Sheng L, Zhang HK, Gu M, et al. 8,8-Dimethyldihydroberberine with improved bioavailability and oral efficacy on obese and diabetic mouse models. Bioorg Med Chem. 2010;18:5915–24.
36. Turner N, Li JY, Gosby A, To SW, Cheng Z, Miyoshi H, et al. Berberine and its more biologically available derivative, dihydroberberine, inhibit mitochondrial respiratory complex I: a mechanism for the action of berberine to activate AMP-activated protein kinase and improve insulin action. Diabetes. 2008;57:1414–8.
37. Ge HX, Zhang J, Kai C, Liu JH, Yu BY. Regio- and enantio-selective glycosylation of tetrahydroprotoberberines by Gliocladium deliquescens NRRL1086 resulting in unique alkaloidal glycosides. Appl Microbiol Biotechnol. 2012;93:2357–64.
38. Zhao W, Ge H, Liu K, Chen X, Zhang J, Liu B. Nandinine, a derivative of berberine, inhibits inflammation and reduces insulin resistance in adipocytes via regulation of AMP-kinase activity. Planta Med. 2017;83:203–9.
39. Yu X, Yu S, Chen L, Liu H, Zhang J, Ge H, et al. Tetrahydroberberrubine attenuates lipopolysaccharide-induced acute lung injury by down-regulating MAPK, AKT, and NF-κB signaling pathways. Biomed Pharmacother. 2016;82:489–97.
40. Mi G, Liu S, Zhang J, Liang H, Gao Y, Li N, et al. Levo-tetrahydroberberrubine produces anxiolytic-like effects in mice through the 5-HT_{1A} receptor. PLoS One. 2017;12:e0168964.

41. Wang C, Cai Z, Wang W, Wei M, Si X, Shang Y, et al. Piperine regulates glycogen synthase kinase-3β-related signaling and attenuates cognitive decline in D-galactose-induced aging mouse model. J Nutr Biochem. 2020;75:108261.
42. Bai X, Yang C, Jiao L, Diao H, Meng Z, Wang L, et al. LncRNA MIAT impairs cardiac contractile function by acting on mitochondrial translocator protein TSPO in a mouse model of myocardial infarction. Signal Transduct Target Ther. 2021;6:172.
43. Schnelle M, Catibog N, Zhang M, Nabeebaccus AA, Anderson G, Richards DA, et al. Echocardiographic evaluation of diastolic function in mouse models of heart disease. J Mol Cell Cardiol. 2018;114:20–8.
44. Zhang Y, Jiao L, Sun L, Li Y, Gao Y, Xu C, et al. LncRNA ZFAS1 as a SERCA2a inhibitor to cause intracellular Ca^{2+} overload and contractile dysfunction in a mouse model of myocardial infarction. Circ Res. 2018;122:1354–68.
45. Li HM, Liu X, Meng ZY, Wang L, Zhao LM, Chen H, et al. Kanglexin delays heart aging by promoting mitophagy. Acta Pharmacol Sin. 2022;43:613–23.
46. Zhang Y, Sun L, Xuan L, Pan Z, Hu X, Liu H, et al. Long non-coding RNA CCRR controls cardiac conduction via regulating intercellular coupling. Nat Commun. 2018;9:4176.
47. Wang Q, Qian Y, Wang Q, Yang YF, Ji S, Song W, et al. Metabolites identification of bioactive licorice compounds in rats. J Pharm Biomed Anal. 2015;115:515–22.
48. Rodriguez-Enriquez S, Kai Y, Maldonado E, Currin RT, Lemasters JJ. Roles of mitophagy and the mitochondrial permeability transition in remodeling of cultured rat hepatocytes. Autophagy. 2009;5:1099–106.
49. Mechanick JI, Farkouh ME, Newman JD, Garvey WT. Cardiometabolic-based chronic disease, adiposity and dysglycemia drivers: JACC state-of-the-art review. J Am Coll Cardiol. 2020;75:525–38.
50. Kim HL, Lim WH, Seo JB, Chung WY, Kim SH, Kim MA, et al. Association between arterial stiffness and left ventricular diastolic function in relation to gender and age. Medicine. 2017;96:e5783.
51. Shirakabe A, Ikeda Y, Sciarretta S, Zablocki DK, Sadoshima J. Aging and autophagy in the heart. Circ Res. 2016;118:1563–76.
52. Mohammed SF, Mirzoyev SA, Edwards WD, Dogan A, Grogan DR, Dunlay SM, et al. Left ventricular amyloid deposition in patients with heart failure and preserved ejection fraction. JACC Heart Fail. 2014;2:113–22.
53. Johnson SC, Sangesland M, Kaeberlein M, Rabinovitch PS. Modulating mTOR in aging and health. Interdiscip Top Gerontol. 2015;40:107–27.
54. Harrison DE, Strong R, Sharp ZD, Nelson JF, Astle CM, Flurkey K, et al. Rapamycin fed late in life extends lifespan in genetically heterogeneous mice. Nature. 2009;460:392–5.
55. Blagosklonny MV. Rapamycin for longevity: opinion article. Aging. 2019;11:8048–67.
56. Eisenberg T, Abdellatif M, Schroeder S, Primessnig U, Stekovic S, Pendl T, et al. Cardioprotection and lifespan extension by the natural polyamine spermidine. Nat Med. 2016;22:1428–38.
57. Bonkowski MS, Sinclair DA. Slowing ageing by design: the rise of NAD^+ and sirtuin-activating compounds. Nat Rev Mol Cell Biol. 2016;17:679–90.
58. Mills KF, Yoshida S, Stein LR, Grozio A, Kubota S, Sasaki Y, et al. Long-term administration of nicotinamide mononucleotide mitigates age-associated physiological decline in mice. Cell Metab. 2016;24:795–806.
59. Yoshino J, Baur JA, Imai SI. NAD^+ intermediates: the biology and therapeutic potential of NMN and NR. Cell Metab. 2018;27:513–28.
60. Pieper AA, Xie S, Capota E, Estill SJ, Zhong J, Long JM, et al. Discovery of a proneurogenic, neuroprotective chemical. Cell. 2010;142:39–51.
61. Torregrosa-Muñumer R, Vara E, Fernández-Tresguerres J, Gredilla R. Resveratrol supplementation at old age reverts changes associated with aging in inflammatory, oxidative and apoptotic markers in rat heart. Eur J Nutr. 2021;60:2683–93.
62. Onishi M, Okamoto K. Mitochondrial clearance: mechanisms and roles in cellular fitness. FEBS Lett. 2021;595:1239–63.
63. Bravo-San Pedro JM, Kroemer G, Galluzzi L. Autophagy and mitophagy in cardiovascular disease. Circ Res. 2017;120:1812–24.
64. Ikeda Y, Shirakabe A, Brady C, Zablocki D, Ohishi M, Sadoshima J. Molecular mechanisms mediating mitochondrial dynamics and mitophagy and their functional roles in the cardiovascular system. J Mol Cell Cardiol. 2015;78:116–22.
65. Li Y, Ma Y, Song L, Yu L, Zhang L, Zhang Y, et al. SIRT3 deficiency exacerbates p53/Parkin-mediated mitophagy inhibition and promotes mitochondrial dysfunction: Implication for aged hearts. Int J Mol Med. 2018;41:3517–26.